

# Proton-Transfer Processes in Thiourea: UV Induced Thione $\rightarrow$ Thiol Reaction and Ground State Thiol $\rightarrow$ Thione Tunneling

Hanna Rostkowska, Leszek Lapinski, Artem Khvorostov, and Maciej J. Nowak\*

*Institute of Physics, Polish Academy of Sciences, Al. Lotnikow 32/46, 02-668 Warsaw, Poland*

*Received: March 17, 2003*

Thiourea monomers isolated in a low-temperature argon matrix adopt exclusively the thione tautomeric form. Upon UV ( $\lambda > 300$  nm) irradiation a photoreaction converting the initial isomer of the compound into its thiol tautomer occurred. Two structures of the photoproduct (with syn and anti orientation of the imino C=N–H group with respect to the C–S bond) were identified in the matrix. Subsequently, a back reaction transforming the thiol form into the initial thione tautomer was observed for the matrix kept at 10 K and in darkness. The molecules with the anti conformation underwent this process, whereas those in the syn form remained unchanged. The only possible mechanism of the ground-state thiol  $\rightarrow$  thione transformation at low temperature is proton-tunneling through the very high energy barrier of  $9030\text{ cm}^{-1}$  ( $108\text{ kJ mol}^{-1}$ ) (calculated at the MP2/6-31++G(d,p) level). The experimentally obtained time constant of this process was 52 h. The structure of the photoproduct species was identified by comparing the experimental IR spectra with the theoretically calculated spectra obtained at the DFT(B3LYP)/6-31++G(d,p) level. UV-induced thione  $\rightarrow$  thiol reaction of thiourea as well as the ground-state thiol  $\rightarrow$  thione proton tunneling in the absence of light are reported for the first time.

## Introduction

The photochemistry of thiocarbonyl compounds has been the subject of intensive studies over the recent decades.<sup>1,2</sup> The addition of excited thiones to olefins or dienes, addition to acetylenes, photodimerization, and photooxidation are among the most investigated classes of thione photoreactions. Also intermolecular and intramolecular hydrogen abstraction are the classic photoreactions of the thiocarbonyl group, and the majority of the intramolecular photoreactions of thione compounds belong to this type. Only a few cases of  $\alpha$ -cleavage reactions are known and all of them concern opening of strained rings. In the intramolecular hydrogen atom abstraction reactions, a proton is usually transferred from  $\delta$ -,  $\gamma$ -,  $\beta$ -, or  $\epsilon$ -positions, with respect to the thiocarbonyl group.

Several cases of UV-induced intramolecular proton-transfer reactions from the NH group in the  $\alpha$ -position were found in our laboratory for matrix-isolated thione heterocyclic compounds: 2(1*H*)-pyridinethione,<sup>3</sup> 4(3*H*)-pyrimidinethione,<sup>4</sup> 3(2*H*)-pyridazinethione,<sup>4</sup> 2(1*H*)-quinolinethione,<sup>5</sup> 2,4-dithiouracil,<sup>6</sup> and 2,6-dithiopurine.<sup>7</sup> No other examples of such thione  $\rightarrow$  thiol reactions were known until very recently, when a photoreaction converting the thione form of thioacetamide into the thiol isomer was discovered.<sup>8</sup> The last finding demonstrates that the photo-tautomeric reaction can occur not only for heterocyclic compounds but also for small thioamides.

In the current paper, we report a UV-induced intramolecular thione  $\rightarrow$  thiol proton-transfer reaction in another simple thioamide: thiourea. The second proton-transfer process, observed within the present work, is proton tunneling occurring in the absence of light.

Proton tunneling in the ground electronic state was observed for various molecules.<sup>9</sup> The classic examples are the inversion

of ammonia,<sup>10</sup> hindered rotations of the methyl group,<sup>11</sup> and proton transfer along the intramolecular hydrogen bond in malonaldehyde<sup>12</sup> and tropolone.<sup>13</sup> In the majority of the investigated cases, the structures before and after tunneling are indistinguishable and the potential energy surface is symmetric with respect to the minimum energy path coordinate.

As far as proton-tunneling processes transforming a molecule into its structurally different isomer are concerned, Pettersson et al.<sup>14</sup> recently reported a cis–trans conversion in formic acid. In the first step of that experiment, the cis form of the matrix-isolated formic acid monomers was photogenerated. Subsequently, the more stable trans form of the compound was repopulated in the absence of light by proton tunneling through a  $2800\text{ cm}^{-1}$  barrier. The time scale of such conversion was several minutes.

In the current work, the proton tunneling reaction converting, in a time scale of days, the photoproduct thiol form into the thione tautomer of thiourea was observed. The unusually low rate of this process is caused by the considerably higher (ca.  $9000\text{ cm}^{-1}$ ) barrier for the thiol  $\rightarrow$  thione transition. It is the first experimental observation of proton tunneling through such a high barrier in a matrix-isolated molecule.

## Experimental Section

Thiourea used in this study was a commercial product (Aldrich). A sample of the compound was electrically heated in a miniature glass oven placed in the vacuum chamber of a continuous flow helium cryostat. The vapors of the compound were deposited together with a large excess of argon on a CsI window cooled to 10 K. Argon of spectral purity was supplied by Linde AG. Infrared spectra were recorded, in the range  $4000\text{--}190\text{ cm}^{-1}$  and at  $0.5\text{ cm}^{-1}$  resolution using a Thermo Nicolet Nexus FTIR spectrometer equipped with KBr or “solid substrate” beam splitters and DTGS detectors. Integral intensities of the IR absorption bands were measured by numerical integration.

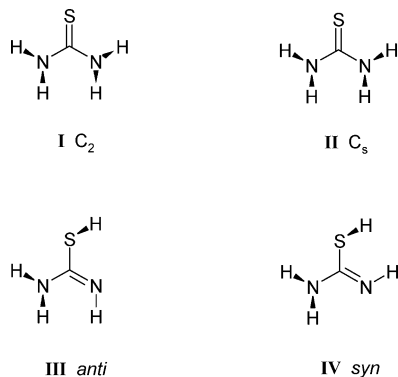
\* To whom correspondence should be addressed. E-mail: mjanow@ifpan.edu.pl.

**TABLE 1: Experimental Wavenumbers ( $\tilde{\nu}$ ) and Relative Integral Intensities ( $I$ ) of the IR Absorption Bands in the Spectrum of Thiourea Isolated in an Argon Matrix and the Assignment to the Normal Modes Calculated for Form I**

experimental		DFT(B3LYP)/6-31++G(d,p) calculated				
$\tilde{\nu},^a \text{ cm}^{-1}$	$I$	mode no.	$\tilde{\nu},^b \text{ cm}^{-1}$	$A^{\text{th}}, \text{ km mol}^{-1}$	symmetry	approximate description <sup>c</sup>
3539	119	Q1	3564	24	A	NH <sub>2</sub> stretching antisym
		Q2	3563	71	B	NH <sub>2</sub> stretching antisym
3424	42	Q3	3434	12	A	NH <sub>2</sub> stretching sym
3418	73	Q4	3426	48	B	NH <sub>2</sub> stretching sym
1610	73	Q5	1609	84	A	NH <sub>2</sub> scissoring
1590	249	Q6	1584	234	B	NH <sub>2</sub> scissoring
<i>1583</i>						
<i>1581</i>						
1518	5					
1401	125	Q7	1384	111	B	CN stretching
<i>1398</i>						
<i>1389</i>						
1385	339	Q8	1366	331	A	NH <sub>2</sub> rocking
1192	4					
1078	6					
1043	72	Q9	1033	66	A	CN stretching
1024	13	Q10	1030	16	B	NH <sub>2</sub> rocking
760	16	Q11	741	13	A	C=S stretching
712	40					
645	29					
577	27					
564	4					
556	6					
507	29					
459	14	Q15	446	5	A	NCN bending
394	41					
<i>284</i>						
282	292					

<sup>a</sup> The frequencies of the subbands are italic. <sup>b</sup> Theoretical frequencies have been scaled by 0.96 (in the range 3600–2000 cm<sup>-1</sup>) and by 0.97 (in the range 2000–200 cm<sup>-1</sup>); A<sup>th</sup> - theoretical absolute intensities. <sup>c</sup> Detailed potential energy distribution (PED) description of the normal modes calculated for form **I** is given in Table S2 of the Supporting Information.

### CHART 1: Isomers of Thiourea



Matrixes were irradiated with light from the HBO200 high-pressure mercury lamp fitted with a water filter and a cutoff filter transmitting light with  $\lambda > 300 \text{ nm}$  or  $\lambda > 270 \text{ nm}$ . The irradiation time was 75 min.

### Computational

The geometries of the structures considered in this work (Chart 1) were optimized using MP2 level ab initio calculations and with density functional theory using Becke's three-parameter exchange functional and gradient-corrected functional of Lee, Yang, and Parr (DFT(B3LYP)). All quantum-mechanical calculations were performed using the GAUSSIAN 98 program.<sup>15</sup> The standard 6-31++G(d,p) basis set was applied in all cases. At the optimized geometries the DFT(B3LYP) harmonic vibrational frequencies and IR intensities were calculated. To correct for the systematic shortcomings of the applied methodology, the predicted vibrational wavenumbers were scaled down

by 0.96 (in the range 4000–2000 cm<sup>-1</sup>) or 0.97 (in the range 2000–200 cm<sup>-1</sup>). The standard potential energy distribution (PED) analysis<sup>16</sup> of the calculated normal modes was performed. Internal coordinates used in this analysis are given in Tables S1 and S3 (Supporting Information). The PED matrix elements greater than 10% are listed in Tables S2, S4, and S5 (Supporting Information).

### Results and Discussion

**Thiourea in Ar Matrix.** The thione tautomer **I** of thiourea (see Chart 1) is by far the most stable form of the compound. The internal energy difference between this form and the thiol tautomer **III** (calculated in the present work at the MP2/6-31++G(d,p) level and corrected for zero-point vibrational energy) is 55 kJ mol<sup>-1</sup>, in favor of **I**. (The relative energies of four conformers of thiol tautomer of thiourea are given in Table S6.) Hence, only the molecules of thiourea in the thione tautomeric form should be expected in a low-temperature inert gas matrix. The infrared spectrum of thiourea isolated in a low-temperature Ar matrix is shown in Figure 1B and compared with the theoretically (DFT(B3LYP)/6-31++G(d,p)) calculated spectrum of the thione form **I** (Figure 1A). The frequencies and intensities of the observed IR bands are collected in Table 1 together with the assignments to the theoretically predicted normal modes.

The bands corresponding to the NH stretching vibrations were observed in the 3600–3300 cm<sup>-1</sup> region. Different coupling of the stretching vibrations of the four NH bonds give rise to four predicted normal modes. In the two higher frequency modes, the atoms perform vibrations antisymmetric with respect to the local symmetry of each of the amino groups. The theoretically calculated frequencies of these modes are practi-

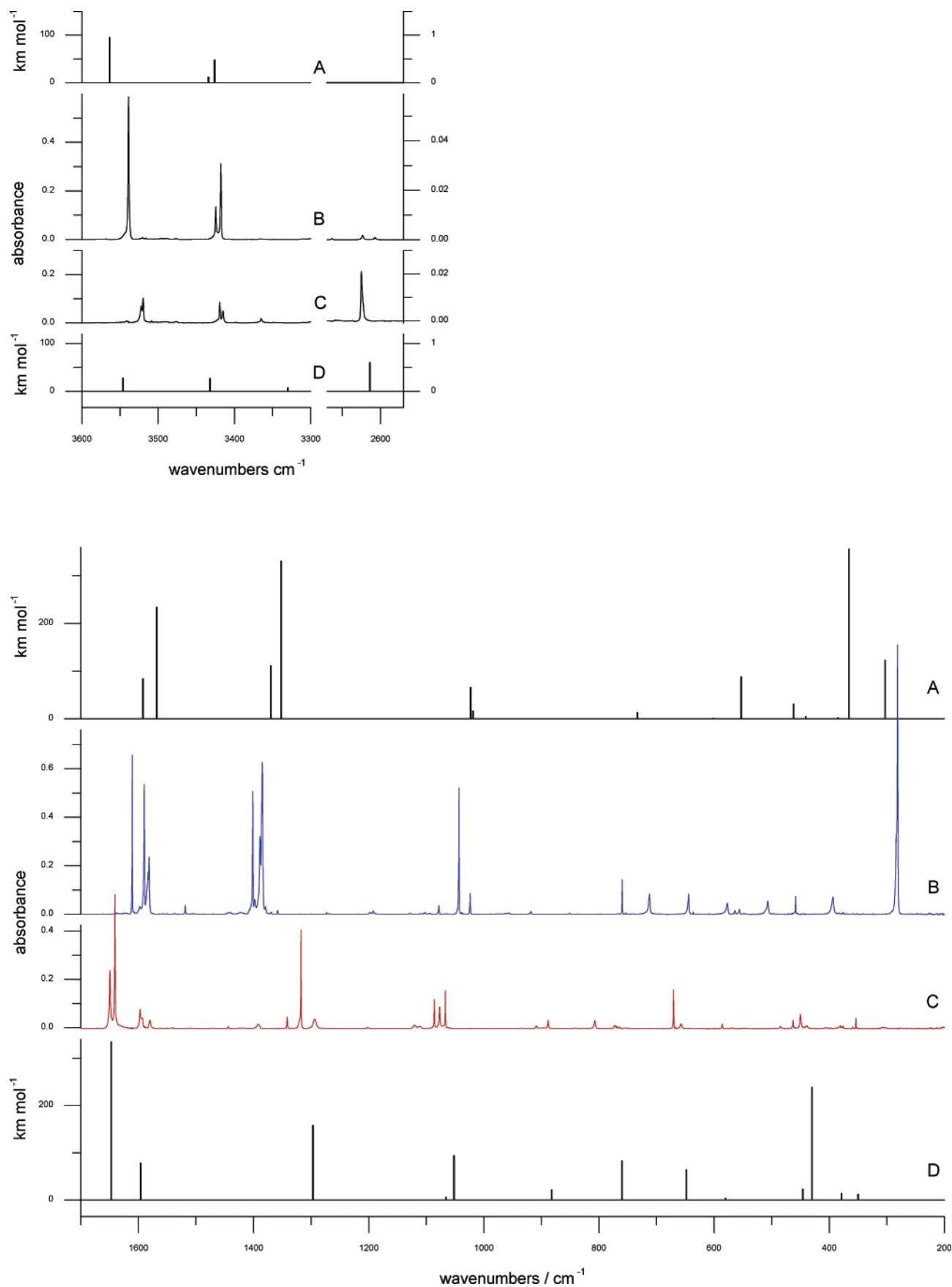


**Figure 1.** (A) Infrared spectrum of the thione tautomer **I** of thiourea calculated at the DFT(B3LYP)/6-31++G(d,p) level. (B) Experimental spectrum of thiourea isolated in an Ar matrix. (C) Experimental spectrum recorded after 75 min of UV ( $\lambda > 270$  nm) irradiation of the matrix. (D) Spectrum of the isomer **III** of the thiol tautomer of thiourea calculated at the DFT(B3LYP)/6-31++G(d,p) level. The baseline of the experimental spectra was corrected; theoretically calculated frequencies were scaled by 0.96 (in the range 4000–2000  $\text{cm}^{-1}$ ) or 0.97 (in the range 2000–200  $\text{cm}^{-1}$ ).

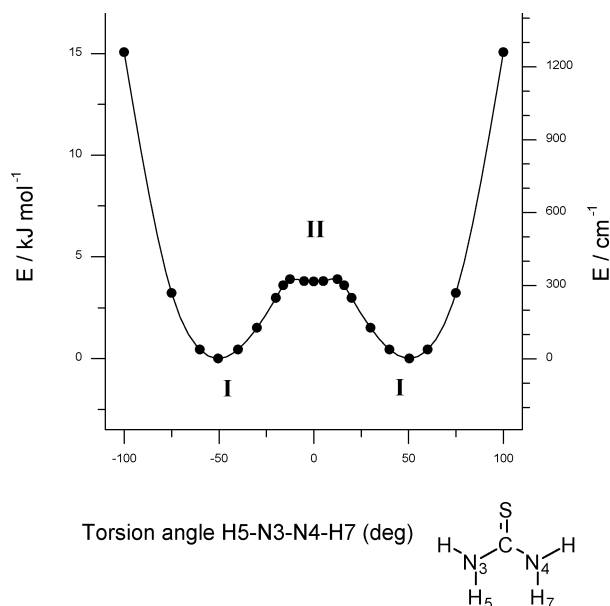


**Figure 2.** The MP2/6-31++G(d,p) potential energy curve for interconversion between the two  $C_2$  equilibrium forms **I** of thiourea via a series of constrained values of the dihedral angle H5–N3–N4–H7 and with the structure fully optimized in all other degrees of freedom. At all intermediate points the  $C_2$  symmetry is not conserved. The height of the barrier is  $3.8 \text{ kJ mol}^{-1}$  ( $318 \text{ cm}^{-1}$ ). The shallow minimum ( $11 \text{ cm}^{-1}$  deep) at the top of the barrier corresponds to structure **II** with lone electron pairs of both amino groups on the same side of the heavy atom plane ( $C_s$  symmetry).

cally identical, at  $3564$  and  $3563 \text{ cm}^{-1}$ . In the experimental spectrum of thiourea, the bands due to these modes overlap and are observed as a single band at  $3539 \text{ cm}^{-1}$ . The other two bands, due to  $\text{NH}_2$  stretching vibrations symmetric with respect to local symmetry of each  $\text{NH}_2$  group, are theoretically predicted at  $3434$  and  $3426 \text{ cm}^{-1}$ . Accordingly, two experimental bands, separated by  $6 \text{ cm}^{-1}$  were found in the experimental spectrum at  $3424$  and  $3418 \text{ cm}^{-1}$ .

The general pattern of the experimental spectrum is fairly well reproduced by the theoretical spectrum. This is the case not only in the  $3600\text{--}3300 \text{ cm}^{-1}$  region but also in the frequency range  $1700\text{--}850 \text{ cm}^{-1}$  (Figure 1) and supports the assignment of the initially deposited form of thiourea to the thione tautomer **I**.

At frequencies lower than  $850 \text{ cm}^{-1}$ , where bands due to the torsional vibrations of the hydrogen atoms in the amino groups are present, the agreement between theory and experiment is much worse. The molecule of thiourea, in its thione form **I**, is not planar; both amino groups are pyramidal. The ground conformational state of the thione tautomer of thiourea has overall  $C_2$  symmetry. Inversion of both amino groups leads to the second, symmetry identical minimum (see Figure 2). Such a double minimum shape of the potential energy hypersurface is significantly different from that assumed in the harmonic approximation. The low-frequency vibrations cannot be well described in the calculation carried out within the model of harmonic vibrations performed by a molecule within a single potential energy well. This explains the differences between the experimental and theoretical spectra in the low-frequency range.

**UV-Induced Thione  $\rightarrow$  Thiol Reaction.** Upon UV ( $\lambda > 270 \text{ nm}$ ) irradiation of the matrix the initial spectrum disappeared completely, while new bands of the IR spectrum of photoproduct(s) emerged. The spectrum recorded after 75 min of UV irradiation is presented in Figure 1C. Exactly the same spectrum of the photoproduct(s) was obtained in another experiment, in

which UV ( $\lambda > 300 \text{ nm}$ ) light was used for irradiation of the matrix. One of the important characteristics of the new spectrum is the band at  $2625 \text{ cm}^{-1}$  (Ar). This frequency is typical of bands due to stretching vibrations of SH groups.<sup>3,8,17</sup> Appearance of this band (see Figure 1C) suggests that the photoproduct is a thiol form of thiourea, produced by photoinduced proton transfer from one of the nitrogen atoms to sulfur. The DFT(B3LYP)/6-31++G(d,p) calculated spectrum of the thiol form **III** (trace D) is compared in Figure 1 with the experimental spectrum recorded after UV irradiation (see also Table 2). In the frequency range  $3600\text{--}850 \text{ cm}^{-1}$ , the general pattern of the experimental spectrum is quite well reproduced by the theoretical spectrum obtained within the harmonic approximation. The new bands observed at  $3523$ ,  $3520$  and  $3419$ ,  $3415 \text{ cm}^{-1}$  should be assigned to the antisymmetric and symmetric vibrations of the only amino group present in the thiol tautomer. Their intensities are several times lower than those of the NH stretching bands in the initial spectrum. According to the calculations, the intensities of these bands in the spectrum of the thiol form should be considerably (2–4 times) weaker than the intensities of the  $\nu(\text{NH}_2)$  bands in the spectrum of the initial, thione form (Tables 1 and 2). The observation that both  $\nu(\text{NH}_2)$  bands, appearing in the spectrum recorded after UV irradiation, are split into two components suggests that two conformations of the thiol photoproduct are stabilized in the Ar matrix. This possibility will be analyzed in detail in the next section.

The comparison between the low-frequency (below  $850 \text{ cm}^{-1}$ ) region of the calculated spectrum of the thiol tautomer of thiourea and the experimental spectrum that emerged after UV irradiation neither supports nor excludes the presence of the thiol structure of the photoproduct. The slightly pyramidal amino group in the thiol form of thiourea endows this species with a double minimum potential well. Hence, as in the case of the thione tautomer, no agreement between the low-frequency fragments of the experimental spectrum and that calculated within the single minimum approximation should be expected also for the thiol form.

**Thiol  $\rightarrow$  Thione Proton Tunneling.** The UV-irradiated matrixes, in which the initial form of thiourea was completely transformed to the photoproduct, were subsequently kept for 24 h in darkness and at 10 K. The infrared beam of the FTIR spectrometer and the HeNe laser beam were blocked during this period, except once every 3 h when infrared spectra were recorded. A very slow but systematic decrease of the IR bands of the photoproduct was observed. This was accompanied by a slow recovery of the spectrum of the thione tautomer (Figure 3). During the reaction in the absence of light, all bands of the thione form **I** were found to grow at the same rate. The relative intensities of these reappearing bands were the same as in the spectrum of the thione tautomer recorded just after deposition of the matrix.

The photoproduct thiol form of the compound can transform back into the more energetically stable thione isomer only by proton tunneling through the barrier separating the two tautomers. No other mechanism of the observed process seems possible. The MP2/6-31++G(d,p)-calculated value of the barrier height for proton transfer from the thiol tautomer **III** to the thione form **I** is  $108 \text{ kJ mol}^{-1}$  ( $9030 \text{ cm}^{-1}$ ). Such a high barrier definitely rules out any possibility of “over the barrier” proton transfer at cryogenic temperatures of 10 K ( $kT = 0.08 \text{ kJ mol}^{-1}$ ). For matrix-isolated monomeric molecules, any mechanism involving intermolecular proton transfer can be excluded as well. Hence, proton tunneling must be the key mechanism of the observed process.

**TABLE 2: Experimental Wavenumbers ( $\tilde{\nu}$ ) and Relative Integral Intensities ( $I$ ) of the IR Absorption Bands in the Spectrum of the Photoproduct(s) Generated upon UV Irradiation of Thiourea Isolated in an Argon Matrix and the Assignment to the Normal Modes Calculated for Forms **III** and **IV****

form <sup>a</sup>	experimental		DFT(B3LYP)/6-31++G(d,p) calculated		
	$\tilde{\nu}$ , cm <sup>-1</sup>	$I$	$\tilde{\nu}$ , <sup>b</sup> cm <sup>-1</sup>	$A^{\text{th}}$ , km mol <sup>-1</sup>	PED, <sup>c</sup> %
IV	3523	44	3552	36	$\nu_{\text{a}}(\text{NH}_2)$ (99)
III	3520	63	3545	28	$\nu_{\text{a}}(\text{NH}_2)$ (100)
III	3419	38	3432	27	$\nu_{\text{s}}(\text{NH}_2)$ (100)
IV	3415	26	3430	33	$\nu_{\text{s}}(\text{NH}_2)$ (98)
IV	3365	14	3414	13	$\nu(\text{NH})$ (100)
III	3287	5	3330	7	$\nu(\text{NH})$ (100)
III + IV	2625	12	2614	1	$\nu(\text{SH})$ (100)
			2600	3	$\nu(\text{SH})$ (100)
IV	1649	154	1660	313	$\nu(\text{C}=\text{N})$ (68), $\nu(\text{CN})$ (14), $\text{NH}_2\text{scis}$ (11)
III	1640	198	1647	335	$\nu(\text{C}=\text{N})$ (69), $\nu(\text{CN})$ (12), $\text{NH}_2\text{scis}$ (12)
III	1597	52	1597	78	$\text{NH}_2\text{scis}$ (86), $\nu(\text{C}=\text{N})$ (12)
IV	1580	17	1573	76	$\text{NH}_2\text{scis}$ (86), $\nu(\text{C}=\text{N})$ (12).
	1444	3			
	1392	21			
III	1342	14			
III	1318	109	1297	158	$\beta(\text{NH})$ (33), $\nu(\text{CN})$ (24), $\text{NH}_2\text{rock}$ (20), $\beta(\text{NCN})$ (15)
IV	1294	44	1283	221	$\nu(\text{CN})$ (29), $\beta(\text{NH})$ (27), $\text{NH}_2\text{rock}$ (21), $\beta(\text{NCN})$ (15)
IV	1120	16	1105	43	$\text{NH}_2\text{rock}$ (62), $\nu(\text{C}=\text{N})$ (14), $\beta(\text{NH})$ (13)
IV	1112	13			
III	1086	28	1066	6	$\text{NH}_2\text{rock}$ (63), $\beta(\text{NH})$ (16)
IV	1077	44	1063	99	$\beta(\text{NH})$ (55), $\nu(\text{CN})$ (41)
III	1067	36	1051	94	$\beta(\text{NH})$ (45), $\nu(\text{CN})$ (41)
IV	909	7	903	15	$\beta(\text{SH})$ (91)
III	888	15	883	22	$\beta(\text{SH})$ (88)
III	807	23			
III	773	17			
III	671	33	648	64	$\nu(\text{CS})$ (56), $\beta(\text{NCN})$ (23)
IV	658	17	637	39	$\nu(\text{CS})$ (43), $\beta(\text{NCN})$ (33)
III	586	7	580	4	$\gamma(\text{CS})$ (85), $\tau(\text{NH})$ (12)
III	485	7			
III	463	16			
III	450	35			
IV	439	12			
	405	4			
	381	15			
	354	8			
	192	26			

<sup>a</sup> The assignment of the experimental bands to forms **III** and **IV** is based on the effect of proton tunneling. <sup>b</sup> Theoretical frequencies have been scaled by 0.96 (in the range 3600–2000 cm<sup>-1</sup>) and by 0.97 (in the range 2000–200 cm<sup>-1</sup>);  $A^{\text{th}}$  - theoretical absolute intensities. <sup>c</sup> Internal coordinates used in the PED analysis are defined in Table S3; PED's of all the normal modes calculated for forms **III** and **IV** are given in Tables S4 and S5 of the Supporting Information.

The decrease of the IR bands due to the substrate of the tunneling process is presented, as a function of time, in Figure 4. The experimental rate constant was measured from the linear regression of the natural logarithm of these intensities. The obtained value equal to  $5.3 \times 10^{-6} (\pm 1 \times 10^{-7}) \text{ s}^{-1}$  was the same for all decreasing bands. The corresponding time constant is equal to  $52 \pm 1 \text{ h}$ . It has also been verified that exposure of the matrix to the beams of the FTIR spectrometer does not change the rate of this reaction.

The back tunneling process allowed two sets of bands to be distinguished in the spectrum recorded after UV irradiation. When the matrix was kept in darkness, some of the bands were continuously decreasing (with the rate given above), whereas the intensities of the other bands remained unchanged (Figure 5). For instance, in the high-frequency region of the spectrum, where two doublets appeared after UV irradiation at 3523, 3520 and 3419, 3415 cm<sup>-1</sup>, only one component of each doublet (bands at 3520 and 3419 cm<sup>-1</sup>) decreased during the proton-tunneling process (Figure 5). This observation demonstrates that two species were produced upon UV irradiation. Good candidates for these two photoproducts are the *anti*-**III** and *syn*-**IV** isomers of the thiol tautomer of thiourea (see Chart 1). It can be expected that proton tunneling can occur only for a thiol

conformer with the hydrogen atom of the SH group directed toward the lone electron pair of the imino group. Only form **III** has such geometry, suited for the proton tunneling from the sulfur to the nitrogen atom. On the other hand, in form **IV** the hydrogen atom of the imino NH group is directed toward the SH group and this would considerably hinder the tunneling process. Moreover, recovery of the thione tautomer **I** starting from isomer **IV** would additionally require a shift of the imino proton from the syn to the anti position. These considerations lead to the assumption that isomer **III** of the thiol tautomer is the substrate of the tunneling process while isomer **IV** is not involved.

The above assumption is supported by more detailed analysis of several regions of the experimental spectrum where the IR bands of both the reacting and nonreacting isomers are observed. In the first of the  $\nu(\text{NH}_2)$  doublets mentioned above (bands at 3523, 3520 cm<sup>-1</sup>), the lower frequency component belongs to the spectrum of the isomer consumed in the proton tunneling. Theoretical calculations predict the corresponding doublet with the band of form **IV** to lie at higher frequency (3552 cm<sup>-1</sup>) and the band of the form **III** at lower frequency (3545 cm<sup>-1</sup>). For the second of the  $\nu(\text{NH}_2)$  doublets (bands at 3419 and 3415 cm<sup>-1</sup>), only the higher frequency component diminishes during

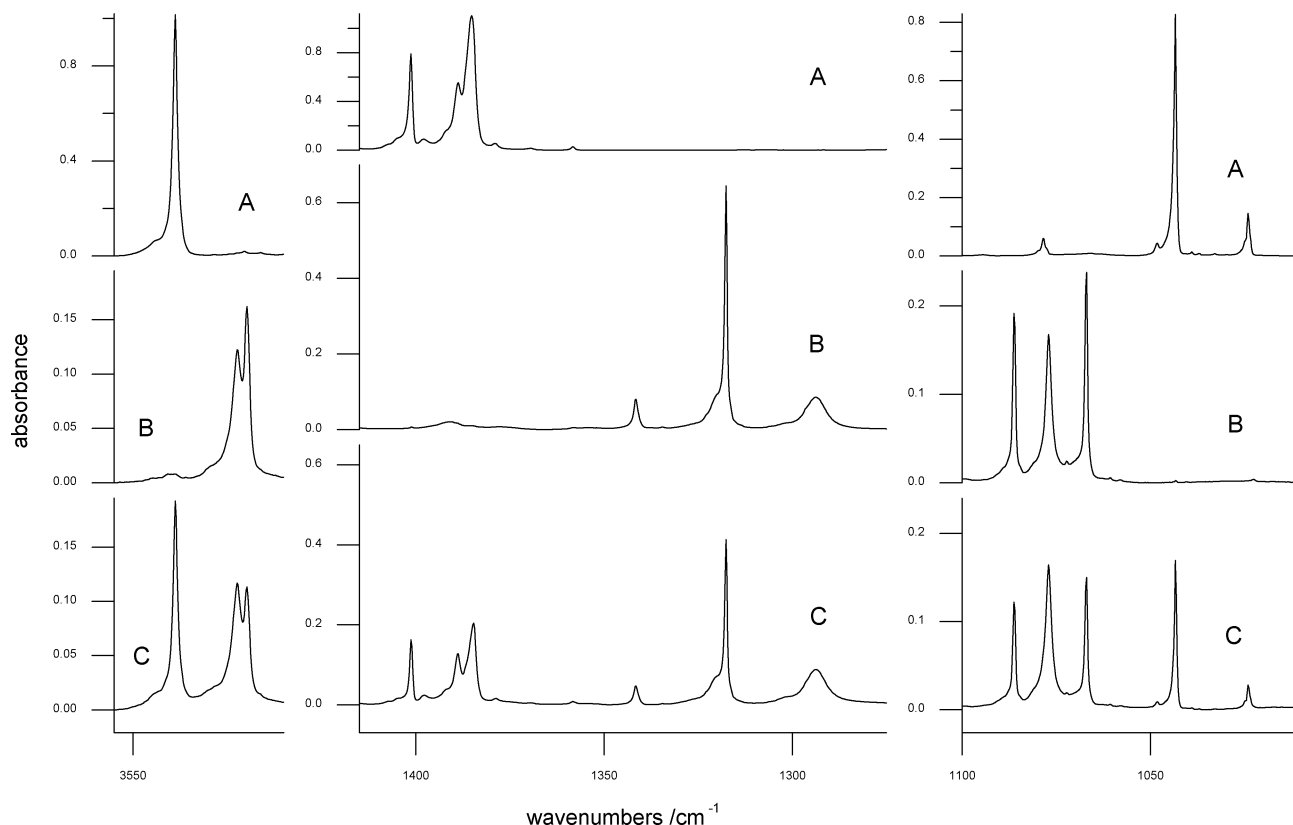


**Figure 3.** Proton tunneling in darkness: (A) initial spectrum of thiourea isolated in an Ar matrix; (B) spectrum of photoproducts generated from Ar-matrix-isolated thiourea upon 75 min of UV ( $\lambda > 270$  nm) irradiation; (C) after 24 h of keeping the matrix in darkness and at 10 K. For traces B and C, the ordinate scales are the same; the ordinate of trace A is reduced.

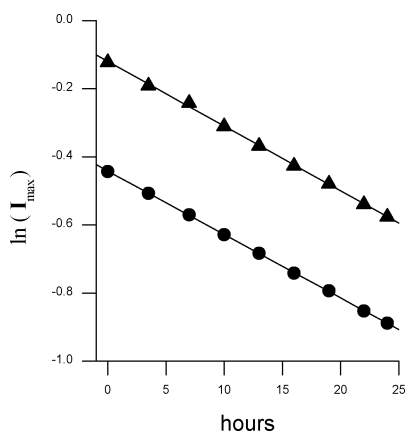


**Figure 4.** Progress of the proton-tunneling process. Natural logarithm of the maximum intensities of the bands at 1640 (triangles) and 1318  $\text{cm}^{-1}$  (full circles), both from the spectrum of form **III** of the thiol tautomer, plotted as a function of time.

the tunneling process (Figure 5). Also in this case the comparison with theoretically predicted frequencies supports the assignment of form **III** to the substrate of the proton tunneling process. In the theoretical spectra the frequency ( $3432 \text{ cm}^{-1}$ ) of the corresponding band of isomer **III** is higher than that of the band calculated for form **IV** ( $3430 \text{ cm}^{-1}$ ).

As a result of different orientations of the imino groups in the syn (**IV**) and anti (**III**) isomers of the thiol tautomer of thiourea, the IR bands due to the  $\nu(\text{NH})$  vibration in this group are theoretically predicted to be of considerably different frequency,  $3414$  (form **IV**) and  $3330 \text{ cm}^{-1}$  (form **III**). The IR intensities of the imino  $\nu(\text{NH})$  bands are usually weak or very weak. Nevertheless, one of the imino  $\nu(\text{NH})$  bands has been clearly detected at  $3365 \text{ cm}^{-1}$  in the spectrum recorded after

UV irradiation. This band did not change its intensity during the tunneling process. A weak band of the form consumed in the proton tunneling has been found in the experimental spectrum at significantly lower frequency,  $3287 \text{ cm}^{-1}$ . These observations support the assignment of form **III** of the thiol tautomer to the substrate of the proton tunneling and of form **IV** to the isomer not involved in this process.

The conclusions reached above are also supported by the analysis of the spectral range  $1700\text{--}1600 \text{ cm}^{-1}$ . Upon UV irradiation two bands due to the stretching of the imino  $\text{C}=\text{N}$  bond appeared in this region at  $1649$  and  $1640 \text{ cm}^{-1}$ . The band at lower frequency decreased during the progress of the proton tunneling in darkness and the intensity of the other band did not change. Again, comparison with the calculated spectra (Figure 5, Table 2), where the  $\nu(\text{C}=\text{N})$  band of isomer **IV** is predicted at higher frequency ( $1660 \text{ cm}^{-1}$ ) than the corresponding band ( $1647 \text{ cm}^{-1}$ ) of isomer **III** suggests the assignment of the substrate of the proton tunneling to the form **III** of thiol tautomer of thiourea.

Finally, the bands corresponding to the bending vibration of the SH group are predicted at frequencies  $903$  (isomer **IV**) and  $883 \text{ cm}^{-1}$  (isomer **III**). In the experimental spectrum, the band decreasing during the tunneling process was observed at  $888 \text{ cm}^{-1}$  and the band unchanged in intensity at  $909 \text{ cm}^{-1}$ . The obvious interpretation of these two bands gives additional confirmation of the assignment of the two photoproducts to forms **IV** and **III** of the thiol tautomer.

Summarizing, comparison of the experimental and theoretical spectra provides sufficient basis for reliable assignment of the species photoproducted from the thione form **I** of thiourea to the anti (**III**) and syn (**IV**) isomers of the thiol tautomer of the compound.

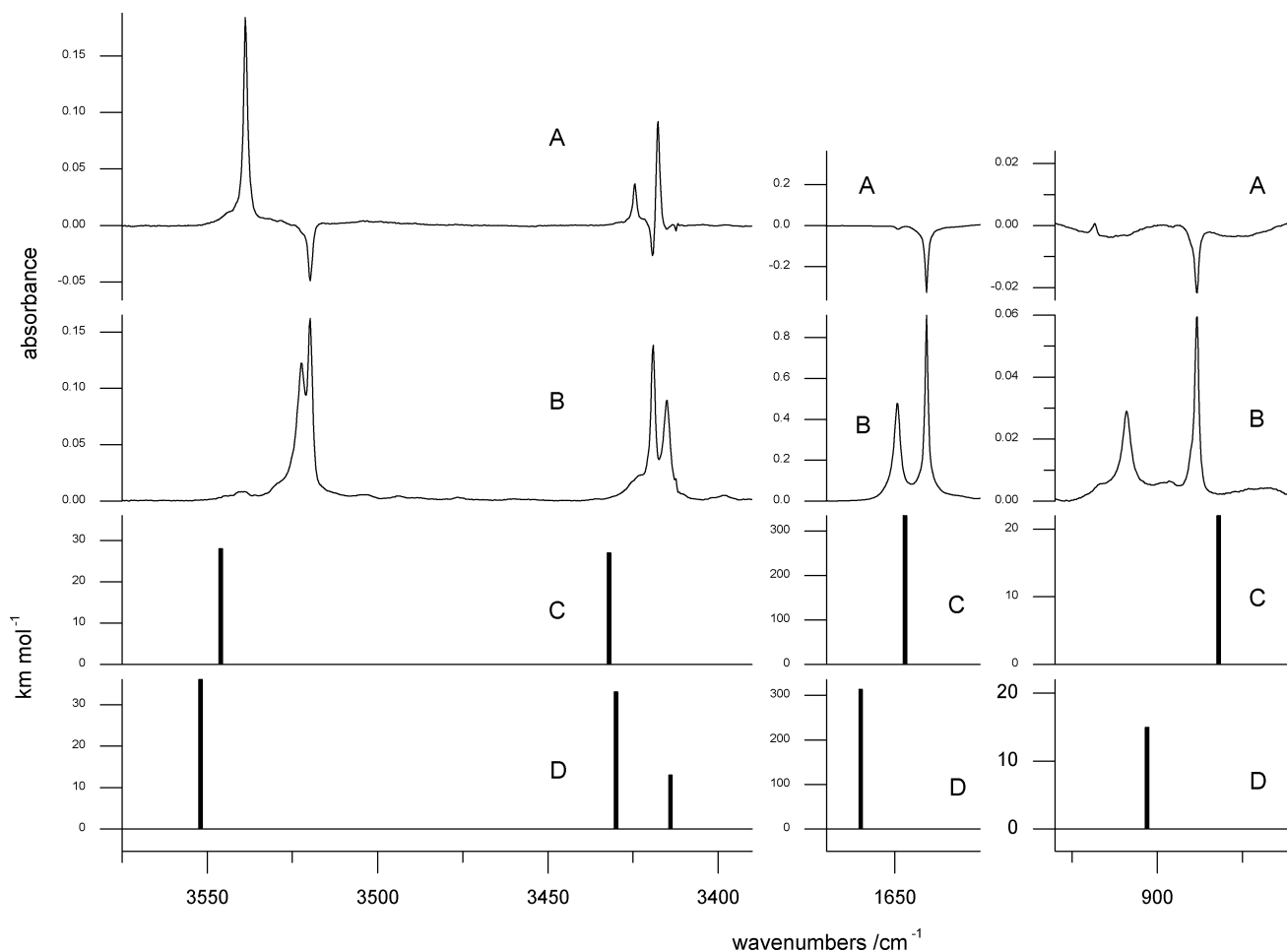
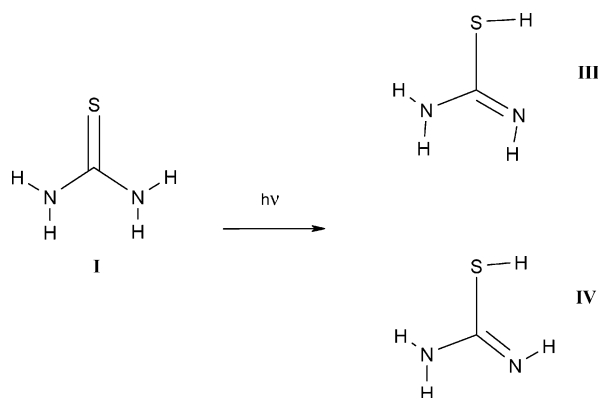


**Figure 5.** (A) Difference between the spectrum recorded after 24 h of keeping the matrix (at 10 K) in darkness and the spectrum of photoproducts (presented as trace B). (B) Spectrum of photoproducts generated from Ar-matrix-isolated thiourea upon 75 min of UV ( $\lambda > 270$  nm) irradiation. (C) Theoretical spectrum of isomer **III** of the thiol tautomer of thiourea. (D) Theoretical spectrum of isomer **IV** of the thiol tautomer of thiourea. The theoretical band at  $3414\text{ cm}^{-1}$  is due to the  $\nu(\text{N-H})$  vibration in the imino group; the corresponding experimental band was observed at  $3365\text{ cm}^{-1}$  (out of the presented range).

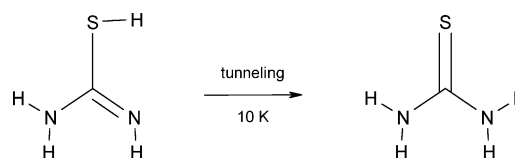
#### SCHEME 1: Phototautomeric Reaction



#### Conclusions

Upon UV irradiation, monomeric thiourea isolated in Ar matrix undergoes a thione  $\rightarrow$  thiol phototautomeric reaction. Two isomers: *anti*-**III** and *syn*-**IV** of the thiol tautomer are photochemically generated in this reaction (Scheme 1). Subsequently, the back thiol  $\rightarrow$  thione proton tunneling process occurs in the absence of light, but only for the anti form **III** (Scheme 2). In contrary to form **IV**, the geometry of form **III** of the thiol tautomer is suitable for proton tunneling from sulfur to the nitrogen atom. The theoretically calculated (MP2) barrier

#### SCHEME 2: Proton Tunneling



for the thiol  $\rightarrow$  thione reaction is as high as  $108\text{ kJ mol}^{-1}$  and the distance between the initial and final position of the proton is  $2.3\text{ \AA}$  (calculated at the MP2 level). Observation of the tunneling process through such a high barrier and with such a long proton-transfer distance is quite unusual for an isolated molecule at cryogenic temperature. The proton-tunneling process in thiourea is the first reported case of a ground-state change of the tautomeric form in a system without intra- or intermolecular hydrogen bonds.

**Supporting Information Available:** Atom numbering of thiourea tautomers is shown in Chart S1. Tables S1 and S3 define the internal coordinates used in the normal-mode analysis for the thione and thiol tautomers of thiourea. Normal modes calculated for isomers **I**, **III**, and **IV** are listed in Tables S2, S4, and S5. Theoretically calculated relative energies of thiourea isomers are given in Table S6. This material is available free of charge via the Internet at <http://pubs.acs.org>.

## References and Notes

- (1) Maciejewski, A.; Steer, R. P. *Chem. Rev.* **1993**, *93*, 67.
- (2) Ramamurthy, V. In *Organic Photochemistry*; Padwa, A., Ed.; Marcel Dekker: New York and Basel, 1985; Vol. 7, Chapter 4.
- (3) Nowak, M. J.; Lapinski, L.; Rostkowska, H.; Les, A.; Adamowicz, L. *J. Phys. Chem.* **1990**, *94*, 7406.
- (4) Nowak, M. J.; Lapinski, L.; Fulara, J.; Les, A.; Adamowicz, L. *J. Phys. Chem.* **1991**, *95*, 2404.
- (5) Prusinowska, D.; Lapinski, L.; Nowak, M. J.; Adamowicz, L. *Spectrochim. Acta* **1995**, *51A*, 1809.
- (6) Lapinski, L.; Nowak, M. J.; Kolos, R.; Kwiatkowski, J. S.; Leszczynski, J. *Spectrochim. Acta* **1998**, *54A*, 685.
- (7) Rostkowska, H.; Lapinski, L.; Nowak, M. J. *J. Phys. Chem. A* **2003**, *107*, 804.
- (8) Lapinski, L.; Rostkowska, H.; Khvorostov, A.; Nowak, M. J. *Phys. Chem. Chem. Phys.* **2003**, *5*, 1524.
- (9) Bell, R. P. *The Tunnel Effect in Chemistry*; Chapman and Hall: London and New York, 1980.
- (10) Dennison, D. M.; Uhlenbeck, G. E. *Phys. Rev.* **1932**, *41*, 313.
- (11) Lin, C. C.; Swalen, J. D. *Rev. Mod. Phys.* **1959**, *31*, 841.
- (12) Tautermann, C. S.; Voegelé, A. F.; Loerting, T.; Liedl, K. R. *J. Chem. Phys.* **2002**, *117*, 1962.
- (13) Redington, R. L. *J. Chem. Phys.* **2000**, *113*, 2319.
- (14) Pettersson, M.; Maçôas, E. M. S.; Khriachtchev, L.; Lundell, J.; Fausto, R.; Räsänen, M. *J. Chem. Phys.* **2002**, *117*, 9095.
- (15) Frisch, M. J.; Trucks, G. W.; Schlegel, H. B.; Scuseria, G. E.; Robb, M. A.; Cheeseman, J. R.; Zakrzewski, V. G.; Montgomery, J. A., Jr.; Stratmann, R. E.; Burant, J. C.; Dapprich, S.; Millam, J. M.; Daniels, A. D.; Kudin, K. N.; Strain, M. C.; Farkas, O.; Tomasi, J.; Barone, V.; Cossi, M.; Cammi, R.; Mennucci, B.; Pomelli, C.; Adamo, C.; Clifford, S.; Ochterski, J.; Petersson, G. A.; Ayala, P. Y.; Cui, Q.; Morokuma, K.; Malick, D. K.; Rabuck, A. D.; Raghavachari, K.; Foresman, J. B.; Cioslowski, J.; Ortiz, J. V.; Baboul, A. G.; Stefanov, B. B.; Liu, G.; Liashenko, A.; Piskorz, P.; Komaromi, I.; Gomperts, R.; Martin, R. L.; Fox, D. J.; Keith, T.; Al-Laham, M. A.; Peng, C. Y.; Nanayakkara, A.; Gonzalez, C.; Challacombe, M.; Gill, P. M. W.; Johnson, B.; Chen, W.; Wong, M. W.; Andres, J. L.; Gonzalez, C.; Head-Gordon, M.; Replogle, E. S.; Pople, J. A. *Gaussian 98*, Revision A.7.; Gaussian, Inc., Pittsburgh, PA, 1998.
- (16) Keresztury, G.; Jalsovszky, G. *J. Mol. Struct.* **1971**, *10*, 304.
- (17) Nowak, M. J.; Rostkowska, H.; Lapinski, L.; Leszczynski, J.; Kwiatkowski, J. S. *Spectrochim. Acta* **1991**, *47A*, 339.